IEEE Transactions on Nuclear Science, Vol.NS-24, No.3, June 1977

LINEAR ACCELERATOR MODELING: DEVELOPMENT AND APPLICATION*

R. A. Jameson and W. E. Jule

Los Alamos Scientific Laboratory
of the University of California
Los Alamos, NM 87545

Summary

Most of the parameters of a modern linear accelerator can be selected by simulating the desired machine characteristics in a computer code and observing how the parameters affect the beam dynamics. The code PARMILA[1] is used at LAMPF for the low-energy portion of linacs. Collections of particles can be traced with a free choice of input distributions in six-dimensional phase space. Random errors are often included in order to study the tolerances which should be imposed during manufacture or in operation.

Once a machine is built, the simulation can be put to another use - that of modeling the actual, observed behavior. If a model of good fidelity can be found, it can be used in many ways: for example, to understand what is happening at intermediate points unobservable in practice. A most important use is to derive optimum settings for the accessible variables. Often the effect of imperfections can be largely alleviated or circumvented once it is realized that they are present and the actual measurements are used in the model. This technique has been successfully applied[2] to the question of longitudinal tuning of the side-coupled linac portion of LAMPF, and is here applied to the same problem in the low-energy portion of the accelerator. We have incorporated as many of the actual measured physical parameters as possible into the code, and have found it necessary to include a more comprehensive treatment of the beam dynamics in order to obtain agreement between the model and experimental observations. The paper outlines the modifications made to the model, the results of experiments which indicate the validity of the model, and the use of the model to optimize the longitudinal tuning of the Alvarez linac.

Introduction

The first cavity, or tank, of the LAMPF linac is a 31-cell, uncompensated, zero-mode Alvarez structure operating at 201.25 MHz, with an axial electric field distribution designed to increase linearly from input to output. There are three more tanks in the Alvarez portion which bring the particles to 100 MeV. Each of these are post-coupler stabilized, with uniform field distributions. All four tanks have a design $\phi_s = -26°$. The linac is preceded by two bunchers, both operating at 201.25 MHz. The phase and amplitude of the rf in these six structures are independently adjustable; the basic problem is how to set these parameters for optimum acceleration characteristics.

The procedure[3] for accomplishing this tuning is to scan an area around the desired operating point, looking for a strongly characteristic pattern which has been predicted by a simulation model. When the pattern is achieved, the model tells how to make the final settings. In this instance, the model and the tune are inextricably interwoven.

It has been observed in practice that the predicted shapes could not be found in detail, although the general features were present. There were indications that the discrepancies occurred in the first tank. Therefore we undertook to experimentally determine the operating characteristics of the 201.25 MHz accelerator and to improve the modeling until agreement was obtained. This report concentrates on the first tank; the results for tanks 2-4 were easier to obtain and are used in developing the final tuning strategy.

Model Development

The Experiment

The goal of the experiment was to map out the longitudinal acceptance of the first tank of the LAMPF 201.25 MHz linac.

Conceptually, the experiment is simple. A monoenergetic, dc beam is transported to the linac. Then the transmission through the first two tanks (with the second tank unexcited) is measured by a copper absorber as a function of the rf amplitude of the first tank (hereafter called an amplitude scan). Then to map out the acceptance it is only necessary to amplitude scan at different injection energies. We did this over a range 720-790 keV (Fig. 1). Finally, we changed the axial electric field distribution (tilt) in tank 1 and repeated the above experiment. We did this for six different tilts.

Each amplitude scan contains information in terms of the amplitude setpoint (ASP) below which there is no transmission (hereafter called the cutoff), and the shape of the curve relating particle transmission to the ASP. From them, we aim at determining the calibration factors which will allow us to set the field to the desired level.

Data Analysis[4]

There are four sets of information to be related: accelerator structure and quadrupole magnet measurements; the experiment data; and the simulation experiment calculated using the PARMILA model.

We have bead pull data for nine different tilts. We chose to do no smoothing to these distributions, but instead to use them exactly as measured. The field level in the tank was controlled at a probe in cell 26, so we normalized all the fields to the design PARMILA value in that cell.

As the data analysis proceeded, it became evident that there was disagreement between the experimental and theoretical data. Since the quad gradients have a strong influence on the dynamics, all of the operating currents were measured. The gradients were entered into the code and a significant part of the disagreement was removed.

To get a preliminary connection between ASP and percent of design field, we did a linear least squares fit to the amplitude scan cutoffs in ASP versus the calculated cutoffs as a percent of design field over the entire energy spectrum for one tilt setting, allowing for an injection energy calibration offset.

The amplitude scan data were manipulated in matrix form using the APL language. Cubic spline smoothing was used, and the curves were extended to allow interpolation over energy. Two types of fitting were necessary.

First it was necessary to relate the experimental transmission to the PARMILA transmission. The correct way to do this would be to measure the current at the entrance of the linac and compare it to the current transmitted through tank 2. This transmission ratio could then be compared directly to the percent of particles transmitted in PARMILA. The transmission at the end of tank 2 was measured but the current measurement at the input of the linac was inaccurate. This

left the relation between experimental and PARMILA transmission indeterminate; the oversight was resolved by normalizing the experimental data to agree with the PARMILA data at 100% of design field for each energy. We then iterated on this normalization by using a gain factor which varied from 0.90 to 1.06 and chose the gain factors which gave the best fit to the data.

The sum of deviations squared was then minimized by searching over energy offsets. The result is an injection energy calibration offset accurate to 0.1 keV, a final linear relation between ASP and field, and a set of transmission gain factors.

The last step necessary to relate the experimental data to the PARMILA data was to relate the experimental tilt to the bead pull tilt conditions by calibrating the movement of the tank heads.

The Model

At the outset of our study, PARMILA included the effects of quadrupole misalignments and measured axial electric field distributions. Artificial phase and energy discrimination were usually used to determine particle transmission. On closer investigation, it was found that very low energy particles were transported through tank 2. This led us to use radial impingement on the drift tubes as the only loss mechanism.

PARMILA allows single as well as multi-particle calculations. Although we are mainly concerned with the longitudinal dynamics, we cannot neglect the transverse influence when simulating actual experiments. Due to computational limitations, it is difficult to do six-dimensional calculations. We circumvented this problem by finding a transverse position which represented the average transverse behavior and using this as an input value in subsequent runs. (For our beam, the transverse space $(x,x',y,y') = (0.2\text{ cm},0,0,0)$ was a good choice.) That is, the transmission cutoffs were nearly the same for the displaced pencil beam as for a beam with a randomly filled transverse phase space.

Actual as-built measurements were used for the longitudinal positioning of drift tubes and drift tube lengths. The gap and cell length errors enter into the calculation of the energy gain per cell:

$$\frac{dW}{dn} = E_0 LT \cos(\phi_s+\Delta\phi)$$

The quantity E_0L is the integral along the axis of the axial electric field. It is obtained from bead pull data and so it is straightforward to include the length errors in the calculation.

The second quantity which is affected is the transit time factor, T. An approximate form for T is

$$T = \frac{\sin(\pi g/L)}{\pi g/L} \quad \frac{I_0(2\pi r/L)}{I_0(2\pi a/L)}$$

where a is the radius of the bore hole. This approximation is poor for determining T, but it is good for determining ΔT. In PARMILA we use

$$T_{PARM} = \frac{T(g+\Delta g, L+\Delta L) - T(g,L)}{T(g,L)} \quad T_{PARM}$$

which is good to 2%.

Finally, straggling effects in the copper absorbers used in the experiments are also taken into account in the PARMILA calculations.

Figure 1 shows a family of amplitude scans for one field tilt setting, assuming an energy offset of 5.8 keV. Figure 2 shows the cutoffs versus energy for six experimental tilts and nine bead pull tilts. The first experimental tilt and the first bead pull tilt match with both heads at mechanical limits. The results match the head calibration as they should. There are two sets of data shown for experimental tilt 1, taken two weeks apart and showing the reproducibility to be within ±1%.

From the above, we feel that our model satisfactorily represents the real linac. In the next section, we will discuss an application of this model to the investigation of a specific question in longitudinal beam dynamics.

Model Application

The Compromise Design

The actual axial electric field distribution as measured by bead pulls varies greatly from the design distribution (Fig. 3) and the large fluctuations in the first few cells drive a large longitudinal oscillation. (The mechanism which is used to produce the tilted field, i.e., changing the gap lengths of only the first and last cells, produces these fluctuations.) The beam gets a 25° kick in the first cell. The goal of our investigation is to determine, for the existing linac, an input phase and energy and a field tilt which would minimize the longitudinal phase oscillation, tail generation, and emittance growth. It is also desirable to have a small ΔE at the end of tank 1, so the subsequent oscillation can be minimized by properly phasing tank 2.

Compromise Design Procedure

The parameter space of energy and phase variation from design $(\Delta E,\Delta\phi)$ and electric field tilt was explored. The aim was to pick a point in this space which would give a small overall phase oscillation in tank 1 and in tank 2. Bead pull tilts 1, 2, and 3 for a region in $(\Delta E,\Delta\phi)$ centered around (8 keV, -25°) satisfied the above criteria and were relatively insensitive, i.e., moving away from the minimum along either axis resulted in only a small increase in the amplitude of the phase oscillation.

The -25° in phase is easy to understand as this is the amount by which the phase is kicked in the first cell. The 8 keV offset gets the beam through the region of the large field fluctuations (the first few cells) with approximately the correct energy to be near the synchronous energy for the remainder of the tank.

In order to refine the choice of parameters, it is necessary to do multi-particle calculations. As a first step, we used a randomly populated elliptical bunch which was ±25° wide and ±10 keV high with no transverse emittance (as we found that transverse emittance had no significant effect on the results) to determine how the emittance developed and how well the beam was matched. These runs showed that -25° was not a good injection point. The beam developed halos and became filamented because one edge of the bunch was too close to the left edge of the acceptance. Moving the beam to -16° gave more cohesiveness and no tails. Tilt 2 gave the best results at this stage; this was satisfying because the field distribution for this tilt is the closest to the design conditions in the center of the tank.

For the last step in determining the optimum operating conditions, we did calculations for a mono-energetic dc beam with no transverse emittance which traversed two bunchers (with no space charge). As noted previously, some particles that are no longer being accelerated will be transported through tank 2. These particles are present in experimental measurements and must be considered. However, they are soon to be lost and thus should not confuse the issue of an optimum tune for the accelerated beam. Hence, we calculate emittance areas for the accelerated particles only and

for all of the particles, and keep track of how many particles are in each area. This gives us quantitative information on cohesiveness and tail generation. On this basis we chose $(\Delta E, \Delta\phi) = (8\ \text{keV}, -16°)$ and tilt 2 as the best operating point.

Some of the outlying particles could be eliminated by lowering the ASP of tank 1 and thus shrinking the acceptance. When the amplitude is lowered it is necessary to shift the input phase to keep $E\cos\phi$ constant. We found that lowering the amplitude by 5% gives the smallest emittance for only a slight loss in transmission, with the fewest particles outside the accelerated core. Further reduction increased the emittance again.

Figures 4-6 show aspects of the final solution. Based on these new operating parameters, PARMILA is used to generate phase scan curves showing the fraction of particles transmitted to the absorber/collector apparatus as functions of the amplitude and phase of the various elements. These phase scans allow us to set the amplitude and rf phase of the two bunchers and the four Alvarez tanks.

Conclusion

It has been demonstrated that modeling of an existing accelerator is possible within the framework of practical beam-dynamics computational tools, and that the model can be of considerable use in understanding observed behavior and finding optimum combinations of the controllable variables.

The model described above was derived and used in an engineering sense, with physical dimensions, fields, and so on, measured as accurately as possible and used directly. The hypothesis of a possible error in the C-W high voltage as read from the voltage divider was necessary to achieve a good fit. In other respects the modeling is straightforward. The model is quite specific to the measurements used; i.e., it is sensitive to measurement errors. However, the insistence upon a global fit to the data and the achievement of it indicate to us that systematic errors have probably been eliminated and that the remaining random errors do not dilute the usefulness of the results. Extension to higher current operation including space charge should now be possible.

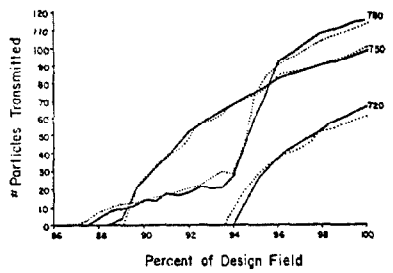

Fig. 1 Experimental (——) and PARMILA (···) generated amplitude scans for tilt 1, at 3 injection energies.

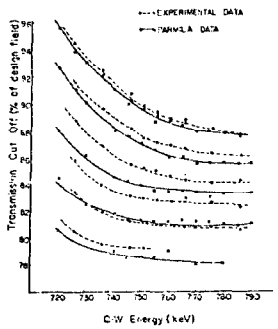

Fig. 2 Cutoffs vs injection energy for several tilts.

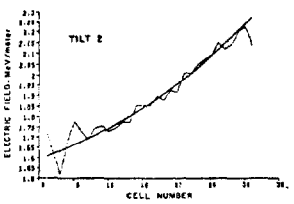

Fig. 3 Design field and actual field from beadpull tilt 2.

Acknowledgments

The capable and dedicated programming assistance from R. S. Mills, and many stimulating discussions with K. R. Crandall and J. S. Stovall, are gratefully acknowledged.

*Work supported by U.S. Energy and Research Development Administration.

[1] Swenson, D. and Stovall, J., "PARMILA," LASL int. doc.
[2] Crandall, K., "Summary of 805 MHz Linac Length Corrections," LASL int. doc.
[3] Swenson, D., "201 Phase Scans," LASL int. doc.
[4] Jameson, R. and Jule, W., "Longitudinal Tuning of the LAMPF 201.25 MHz Linac - Zero Space Charge," to be pub.

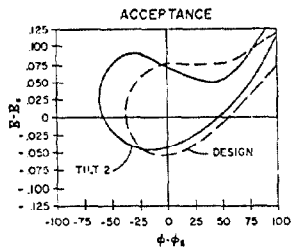

Fig. 4 Design vs actual acceptance of tank 1.

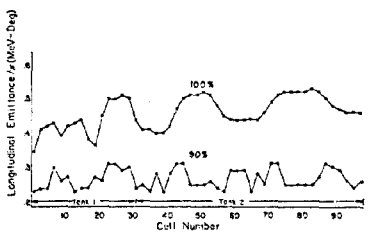

Fig. 5 Calculated longitudinal emittance containing 90% and 100% of particles injected in an ellipse of ±25°, ±10 keV centered at 758 keV and ϕ_s -16°.

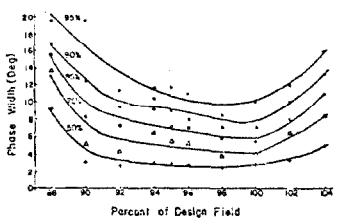

Fig. 6 Actual performance at injection of 756 keV, -42°, showing fraction of beam within phase spread at 40 MeV as function of tank 1 rf field level.